

**TYOLOGY OF COARSE-GRAINED RIPPLES ON MERIDIANI PLANUM, MARS.** J. Kozakiewicz<sup>1</sup>, M. Dluzewski<sup>2</sup>, J. Rotnicka-Dluzewska<sup>3</sup>, M. Sobucki<sup>4</sup>, T. Michaels<sup>5</sup>, M. Pilarska-Mazurek<sup>6</sup>, K. Krzemien<sup>4</sup>, L. Nowak<sup>1</sup>, R. Olszewski<sup>6</sup>, N. Frodyma<sup>1</sup>, A. Podbielska<sup>6</sup>, K. Choromanski<sup>6</sup>. <sup>1</sup>Faculty of Physics, Astronomy, and Applied Computer Science, Jagiellonian University, Krakow, 11 Lojasiewicza St., 30-348, Poland, (j.kozakiewicz@uj.edu.pl). <sup>2</sup>Faculty of Geography and Regional Studies, University of Warsaw, Warsaw, Poland. <sup>3</sup>Faculty of Geographical and Geological Sciences, Adam Mickiewicz University in Poznan, Poznan, Poland. <sup>4</sup>Faculty of Geography and Geology, Jagiellonian University, Krakow, Poland. <sup>5</sup>Space Science and Engineering Center, University of Wisconsin, Madison, Wisconsin, USA. <sup>6</sup>Faculty of Geodesy and Cartography, Warsaw University of Technology, Warsaw, Poland.

**Introduction:** Aeolian coarse-grained ripples [1,2], also called megaripples [3,4], are very common landforms on Mars. Studying these ripples allows us to estimate past and present wind patterns and mechanisms of bedform formation. Previous classifications of ripples on Mars were based on the size of bedforms, given by their wavelength [5], as this is the easiest parameter to measure from orbit, and also on particle size distribution (PSD) if such information was available, as the size of grains in ripples greatly influences ripples' dynamics [6]. In this work, a developed classification of coarse-grained ripples is presented. This classification is based on three factors: i) PSD of ripple surface layers, ii) the size of ripples, given by the wavelength or by the ratio of height to width (the latter parameter can be used for studying solitary bedforms [7]), and iii) ripples' apparent formation context, as many ripples on Mars are shaped by topographically-modified fluid flow.

**Data and Methods:** In order to develop the classification, 448 ripples were measured along the entire 45-km-long traverse of the Opportunity rover. The entire dataset of 200,000 images obtained by the Opportunity rover's Navigation Camera (NAVCAM), Panoramic Camera (PANCAM), Hazard Avoidance Cameras (HAZCAM) as well as the Microscopic Imager (MI) was used. 135 larger bedforms were additionally measured from HiRISE data, as they were hard to observe in their entirety from the rover. DTMs were generated from HiRISE stereopairs using NASA's Ames Stereo Pipeline (ASP) and the Integrated System for Imagers and Spectrometers (ISIS). The final DTM and the orthoimage mosaics covered an area of approximately 87 square km.

**Coarse-grained Ripple Typology:** When Meridiani Planum ripples' PSDs are compared with PSDs obtained during ripple investigations by the rovers in Gale crater [8] and Gusev crater [9], it is clear that there are at least two different populations of ripples on Mars: those made of fine sand and those made of coarse sand (Fig. 1). In this work, these ripples were called fine-grained and coarse-grained ripples, respectively. The fine-grained ripples on MP are quite rare, but the

coarse-grained ripples literally cover the entire area along the Opportunity rover traverse.

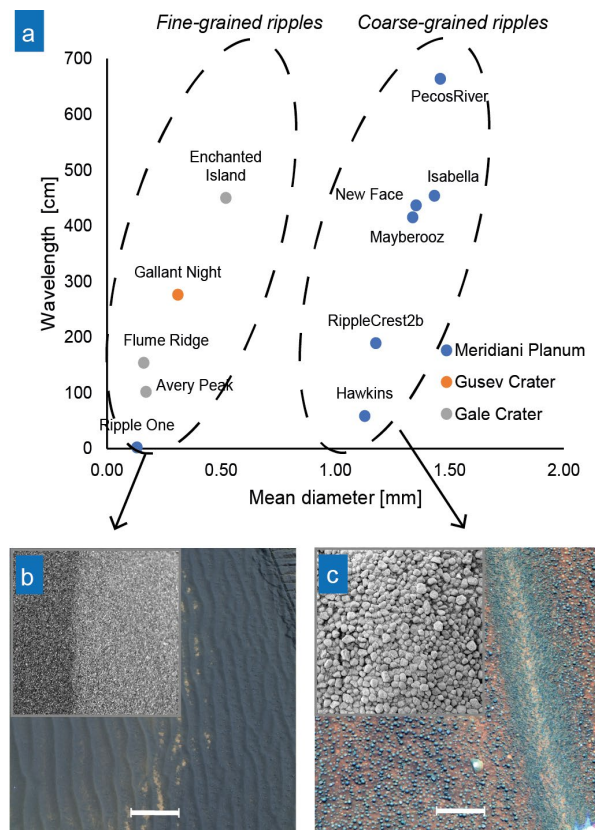


**Figure 1.** (a) The wavelength of ripples vs. the mean diameter of surface grain samples (with target names) for various ripples. Ripples and their surface sands (insets) from MP: (b) fine-grained ripple (sol 0054), (c) coarse-grained ripple (sol 0073). Data from Gale crater after [8] and from Gusev crater after [9]. Scale bars ~10 cm. Both inset images are 3.2 x 3.2 cm.

The ripples' wavelength distribution showed that there are three types of coarse-grained ripples on MP: small, medium, and large (Fig. 2). It was also found that the ripple index (wavelength to height ratio) for all coarse-grained ripples on MP is 15.9, which is similar to the value for coarse-grained ripples on Earth [10].

In several places along the traverse, bedforms composed of coarse sand grains but with atypical morphometry and morphology were observed (Fig. 2). These ripples' occurrence was not random but related to topographical obstacles, such as impact craters, trenches, lineaments, and protrusions. As these atypical ripples were topographically forced, they were called forced ripples as opposed to typical ripples formed by free flow, which were named free ripples. It was observed that the forced ripples' morphology was similar to the morphology of transverse aeolian ridges (TARs). Three types of forced ripples were found on MP: i) rim ripples [11], ii) feathered ripples, and iii) networked ripples [12]. Rim ripples have only one, primary crest and form near small obstacles, such as crater rims or protrusions. Feathered ripples form in large depressions, such as impact craters (simple bedforms) and at low, linear obstacles, such as lineaments (compound bedforms), and have clearly visible primary and secondary crests. Networked ripples are characterized by intertwined primary, secondary, and tertiary crests. They form on the slopes and floors of relatively large depressions, such as impact craters.

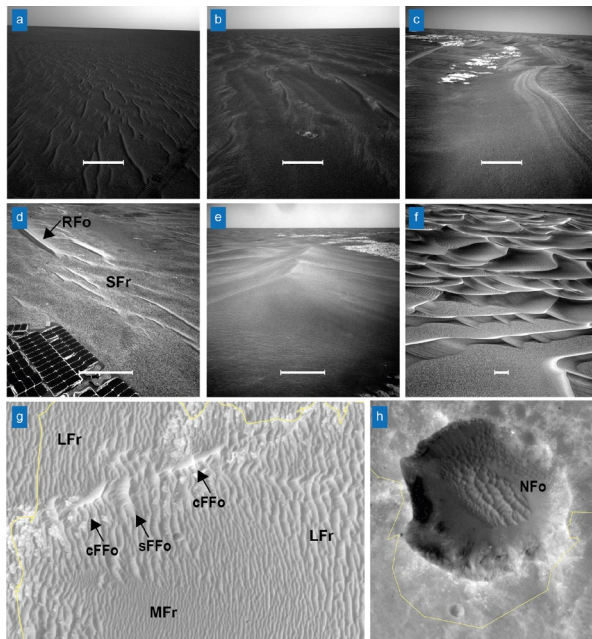


**Figure 2.** Types of coarse-grained ripples on MP. Scale bars - 0.5 m. *Upper row* - free ripples: (a) small ripples (sol 0070); (b) medium ripples (sol 0362); (c) large ripples (sol 0796). *Middle row* - forced ripples: (d) rim ripple (RFo), near the trench, with small free ripples (SFr) in its vicinity (sol 0321); (e) feathered ripple (cFFo) (only a part of the bedform is visible) (sol 1710); (f) networked ripples (NFo) (sol 0198). *Lower row*: (g) simple and compound feathered ripples (sFFo and cFFo) within a field of large free ripples (LFr) and

medium free ripples (MFr) as seen from orbit on the NW rim of Erebus crater (the width of the simple feathered ripple, sFFo is ~16m); (h) coarse-grained forced networked ripples (NFo) on the floor of Santa Maria crater (crater diameter ~90m). Yellow lines - the rover traverse.

**Acknowledgments:** Data used in this study are publicly available via the NASA Geosciences Node of the Planetary Data System ([https://pds-geosciences.wustl.edu/missions/mer/geo\\_mer\\_datasets.htm](https://pds-geosciences.wustl.edu/missions/mer/geo_mer_datasets.htm)) and can be accessed through the MER Analyst's Notebook at <https://an.rsl.wustl.edu/mer/>. NAVCAM [10.17189/1520327](https://doi.org/10.17189/1520327), MI [10.17189/1520416](https://doi.org/10.17189/1520416), PANCAM [10.17189/1520220](https://doi.org/10.17189/1520220), HAZCAM [10.17189/1520235](https://doi.org/10.17189/1520235), HIRISE [10.17189/1520303](https://doi.org/10.17189/1520303).

The work was funded by the Anthropocene Priority Research Area budget under the program "Excellence Initiative – Research University" at the Jagiellonian University, and by POB Research Centre Cybersecurity and Data Science of Warsaw University of Technology within the Excellence Initiative Program - Research University (ID-UB).

#### References:

- [1] Jerolmack D. (2006) *JGR*, 111, E12S02.
- [2] Sullivan R. et al. (2008) *JGR*, 113, E06S07.
- [3] Greeley, R. & Iversen, J.D. (1985) *Wind as a Geological Process on Earth, Mars, Venus, and Titan*. Cambridge University Press.
- [4] Zimbelman, J. R. (2019) *Icarus*, Volume 333, Pages 127–129.
- [5] Lapotre, M. et al. (2016) *Science*, 353(6294), 55–58.
- [6] Day, M. & Zimbelman J. R. (2021) *Icarus*, 369, 114647.
- [7] Zimbelman, J. R. & Foroutan, M. (2020) *JGR*, 125.
- [8] Gough, T. R. et al. (2021) *JGR*, 126, e2021JE007011.
- [9] Cabrol, N. A., et al. (2014) *JGR*, 119, 941–967.
- [10] Sharp R. (1963) *Journal of Geology*, 71, 617–636.
- [11] Sullivan, R. et al. (2007) *LPS XXXVIII*, Abstract #204.
- [12] Nagle-McNaughton, T. P. & Scuderi, L. A. (2021) *Commun. Earth Environ.*, 2, 217.